

Generalization of CNOT-based Discrete Circular Quantum Walk: Simulation and Effect of Gate Errors

Iyed Ben Slimen¹, Amor Gueddana^{2,3} and Vasudevan Lakshminarayanan^{3,4}

1- SysCom Lab, National Engineering School of Tunis, ENIT, University of EL Manar, 1002 Le Belvédère, Tunis, Tunisia

2- Green & Smart Communication Systems Lab, Gres'Com, Engineering School of Communication of Tunis, Sup'Com, University of Carthage, Ghazela Technopark, 2083, Ariana, Tunisia.

3- Theoretical & Experimental Epistemology Lab, TEEL, School of Optometry and Vision Science, University of Waterloo 200 University Avenue West, Waterloo, Ontario N2L 3G1, Canada.

4- Department of Physics, Department of Electrical and Computer Engineering and Department of Systems Design Engineering, University of Waterloo 200 University Avenue West, Waterloo, Ontario N2L 3G1, Canada.

Abstract—We investigate the counterparts of random walk in universal quantum computing and their implementation using standard quantum circuits. Quantum walk have been recently well investigated for traversing graphs with certain oracles. We focus our study on traversing a 1-D graph, namely a circle, and show how to implement discrete circular quantum walk in quantum circuits built with universal CNOT and single qubit gates. We review elementary quantum gates and circuit decomposition and propose a generalized version of the all CNOT based quantum discrete circular walk. We simulated these circuits on an IBM quantum supercomputer London IBM-Q with 5 qubits. This quantum computer has non perfect gates based on superconducting qubits, therefore we analyze the impact of errors on the fidelity of the Walker circuit.

Index Terms—CNOT gate, quantum computing, Quantum random walk

I. INTRODUCTION

Like any other generalized tool in the field of quantum computing, there exists a quantum version of random walk, a useful mathematical tool to model graphs such as Markov chains. Basic concepts of quantum walk can be found in [1]. Quantum walk are used in computer science and are fundamental for building quantum routers. The best examples of quantum algorithms based on quantum walk are the searching in an unsorted list, searching in an hypercube, element distinctness problem, triangle problems etc ... [2]. Circuit implementations of quantum walk along a circle, a 2D hypercycle, a twisted toroidal lattice graph, a complete circle and a glued tree are presented in [3]. Other research has

addressed physical realization of quantum walk algorithms[4]. We distinguish two models of quantum walk: (1). The discrete quantum walk, where we require a coin qubit, a walker qubits and a unitary evolution operator and (2). Continuous quantum walk, where an evolution operator is applied with no restrictions and the time evolution of the walker is given through the Schrödinger equation [1]. In this paper, we address the circuit implementation of all CNOT based Circular Quantum Discrete Random Walk (CQDRW) along a circle and we simulate them on an IBMQ machine. In this work, we use the London 5 qubits IBM-Q to simulate a 4 qubits CQDRW.

This paper is organized into four sections: we start section 2 by reviewing some single quantum gates and the CNOT in order to recall their universality. We also show how to decompose $C^n NOT$ into elementary gates, specifically $C^2 NOT$ and $C^3 NOT$. We show that their simulation on the IBM composer and their implementation on London IBMQ have different outputs due to errors of the gates. Section 3 presents the $CNOT$ based circuits for building CQDRW in a general context. The specific simulation results for the 4 qubits walker is presented in section 4. We focus on comparing the composer simulation and the device execution to study the impact of errors gates mainly due to $CNOT$ s. The analysis is done by calculating the fidelity parameter. We conclude with other possible 2-D quantum walk implementation and some techniques to reduce the set of obtained errors.

II. ELEMENTARY GATES FOR BUILDING QUANTUM CIRCUITS

A. Universality of the CNOT and the single qubit gates

Single qubit gates are the basic elements for building quantum circuit. We address in this work the Identity gate (I_2), the Hadamard gate (H), the negation gate (σ_x), the rotation by θ around \hat{y} ($R_y(\theta)$), the rotation by α around \hat{z} ($R_z(\alpha)$), the δ -phase shift gate ($\Phi(\delta)$) and the $T(\varphi)$ gate, having the following transforms [5], [6], [7]:

$$I_2 = \begin{pmatrix} 1 & 0 \\ 0 & 1 \end{pmatrix} \quad (1)$$

$$H = \frac{1}{\sqrt{2}} \begin{pmatrix} 1 & 1 \\ 1 & -1 \end{pmatrix} \quad (2)$$

$$\sigma_x = \begin{pmatrix} 0 & 1 \\ 1 & 0 \end{pmatrix} \quad (3)$$

$$R_y(\theta) = \begin{pmatrix} \cos\frac{\theta}{2} & \sin\frac{\theta}{2} \\ -\sin\frac{\theta}{2} & \cos\frac{\theta}{2} \end{pmatrix} \quad (4)$$

$$R_z(\alpha) = \begin{pmatrix} e^{i\alpha/2} & 0 \\ 0 & e^{-i\alpha/2} \end{pmatrix} \quad (5)$$

$$\phi(\delta) = \begin{pmatrix} e^{i\delta} & 0 \\ 0 & e^{i\delta} \end{pmatrix} \quad (6)$$

$$T(\varphi) = R_z(-\varphi)\phi\left(\frac{\varphi}{2}\right) = \begin{pmatrix} 1 & 0 \\ 0 & e^{i\varphi} \end{pmatrix} \quad (7)$$

The σ_x gate is also known as the NOT transform as illustrated by figure 1. The Controlled-NOT (CNOT) gate is a two qubits gate, it performs σ_x on the target qubit if and only if the control qubit is in the state $|1\rangle$, it has the following transform:

$$U_{CNOT} = \begin{pmatrix} 1 & 0 & 0 & 0 \\ 0 & 1 & 0 & 0 \\ 0 & 0 & 0 & 1 \\ 0 & 0 & 1 & 0 \end{pmatrix} \quad (8)$$

The set of single qubit gates and CNOT gate are universal for building any quantum circuit. Specifically, any unitary gate acting on multiple qubit circuit can be implemented with single qubit gates and CNOT gates. Following paragraphs, we show how to decompose certain circuits into a set of single qubit and CNOT gates.

The NOT controlled by two qubits is known as the Toffoli gate, having the following transform:

$$U_{Toffoli} = \begin{pmatrix} 1 & 0 & 0 & 0 & 0 & 0 & 0 & 0 \\ 0 & 1 & 0 & 0 & 0 & 0 & 0 & 0 \\ 0 & 0 & 1 & 0 & 0 & 0 & 0 & 0 \\ 0 & 0 & 0 & 1 & 0 & 0 & 0 & 0 \\ 0 & 0 & 0 & 0 & 1 & 0 & 0 & 0 \\ 0 & 0 & 0 & 0 & 0 & 1 & 0 & 0 \\ 0 & 0 & 0 & 0 & 0 & 0 & 0 & 1 \\ 0 & 0 & 0 & 0 & 0 & 0 & 1 & 0 \end{pmatrix} \quad (9)$$

Further generalization of the NOT gate, controlled by n qubits all in the state $|1\rangle$, is referred as C^nNOT gate. When the NOT gate is controlled by the n qubits all in the state $|0\rangle$, it is denoted C_0^nNOT and its control qubits are represented by the empty circle (figure 1).

The matrix transforms of the C^nNOT and the C_0^nNOT are obtained as follows:

$$U_{C^nNOT} = \begin{pmatrix} I_2 & O & . & . & . & O \\ O & I_2 & . & . & . & . \\ . & . & . & . & . & . \\ . & . & . & . & . & . \\ . & . & . & . & I_2 & O \\ O & . & . & . & O & \sigma_x \end{pmatrix} = \begin{pmatrix} I_{2^{n+1}-2} & O \\ O & \sigma_x \end{pmatrix} \quad (10)$$

$$U_{C_0^nNOT} = \begin{pmatrix} \sigma_x & O & . & . & . & O \\ O & I_2 & . & . & . & . \\ . & . & . & . & . & . \\ . & . & . & . & . & . \\ . & . & . & . & I_2 & O \\ O & . & . & . & O & I_2 \end{pmatrix} = \begin{pmatrix} \sigma_x & O \\ O & I_{2^{n+1}-2} \end{pmatrix} \quad (11)$$

where $I_{2^{n+1}-2}$ is a $(2^{n+1}-2) \times (2^{n+1}-2)$ identity matrix.

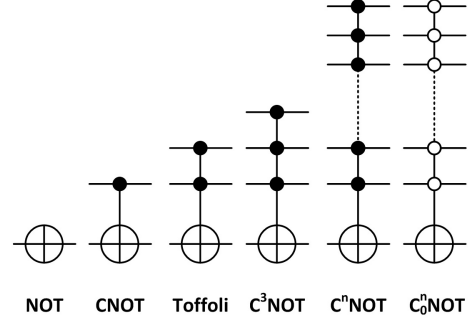


Figure 1: Controlled NOT gates

Many works have addressed circuit implementation of quantum algorithms, such as database search algorithms, while using C^nNOT and C_0^nNOT gates [8], [9], but IBMQ uses only single qubit operations and multiple CNOTs to implement the circuits. Therefore, we show in figure 2 the technique used to build equivalent C^nNOT based implementation of C_0^nNOT gates [10].

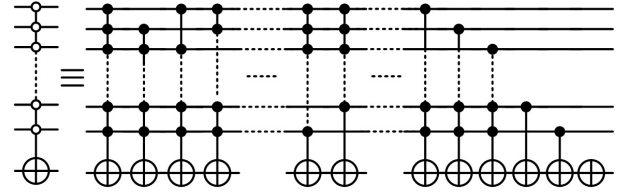
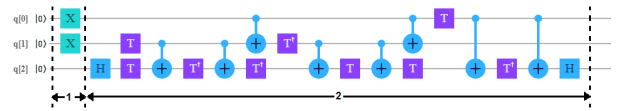


Figure 2: Equivalent C^nNOT based implementation of C_0^nNOT gates

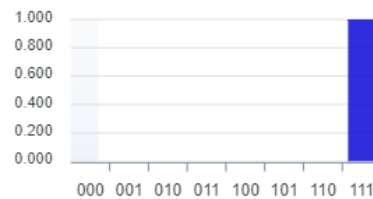
B. CNOT based implementation of C^nNOT gates

Following the general decomposition method described in [11], [12], we illustrate in stage 2 of figure 3a the $CNOT$ based implementation of the Toffoli gate, while the T and T^\dagger transforms refer to $T(\pi/4)$ and $T(-\pi/4)$ of equation 7, respectively.



(a) $CNOT$ based implementation of Toffoli gate.

Statevector



(b) Output corresponding to the input state $|110\rangle$ after simulation on the IBMQ composer

Figure 3: Decomposition of the Toffoli gate and result of simulation in the IBMQ composer for one input $|110\rangle$

For any circuit to be simulated, IBMQ sets all input qubits automatically to 0. In our case, the input of the decomposed Toffoli gate is set by default to $|000\rangle$. To observe the output of the decomposed Toffoli, we consider only the input state $|110\rangle$, to this end, we add the two *NOT* gates in stage 1 of figure 3a (represented by *X* gate in IBMQ), and we illustrate the correct output $|111\rangle$ in figure 3b as obtained after simulation on the composer.

To observe the result after execution on the real IBMQ device, a transpiled circuit is automatically generated as given by figure 4a. The transpiled circuit performs some approximations and simplifications based on optimizations techniques to generate transpiled circuits that are equivalent to the original circuit. For these approximations, all single qubits transforms given by equation 1 to equation 7 are compiled down to physical gates based on superconducting qubits, denoted U_1 , U_2 and U_3 , and given as follows:

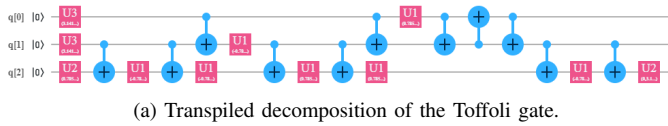
$$U_1(\lambda) = U_3(0, 0, \lambda) = \begin{pmatrix} 1 & 0 \\ 0 & e^{i\lambda} \end{pmatrix} \quad (12)$$

$$U_2(\phi, \lambda) = U_3(\pi/2, \phi, \lambda) = \frac{1}{\sqrt{2}} \begin{pmatrix} 1 & -e^{i\lambda} \\ e^{i\phi} & e^{i\lambda+i\phi} \end{pmatrix} \quad (13)$$

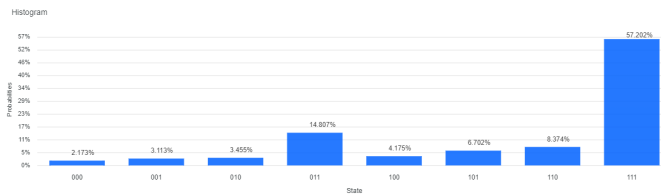
$$U_3(\theta, \phi, \lambda) = \begin{pmatrix} \cos(\theta/2) & -e^{i\lambda} \sin(\theta/2) \\ e^{i\phi} \sin(\theta/2) & e^{i\lambda+i\phi} \cos(\theta/2) \end{pmatrix} \quad (14)$$

From equations 12, 13 and 14, we deduce that the two *NOT*s gates illustrated in stage 1 of figure 3a are implemented by $U_3(\pi, 0, \pi)$, while the Hadamard gate of equation 2 is obtained by $U_2(0, \pi)$.

For the same input state $|110\rangle$ applied to the composer, we illustrate in figure 4b the output after execution on the IBMQ device. We observe a success probability of 57.202 % for obtaining the correct output $|111\rangle$, and various errors for the other output states $|000\rangle$, $|001\rangle$, $|010\rangle$, $|011\rangle$, $|100\rangle$, $|101\rangle$ and $|110\rangle$.

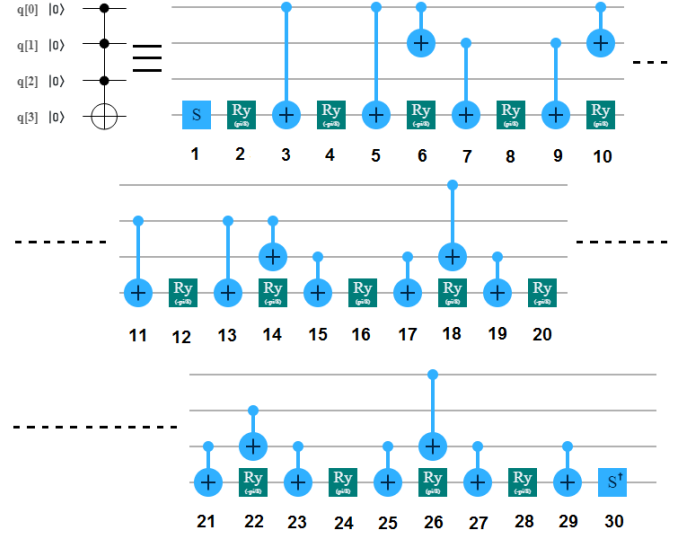


(a) Transpiled decomposition of the Toffoli gate.



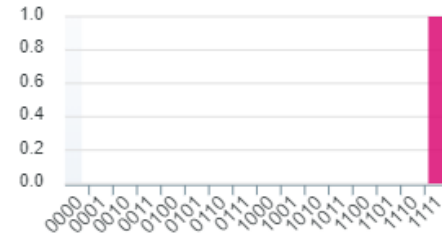
(b) Output corresponding to the input state $|110\rangle$ after execution on the IBMQ device

Figure 4: Transpiled circuit of the *CNOT* based implementation of Toffoli gate.



(a) *CNOT* based implementation of C^3NOT gate.

Statevector

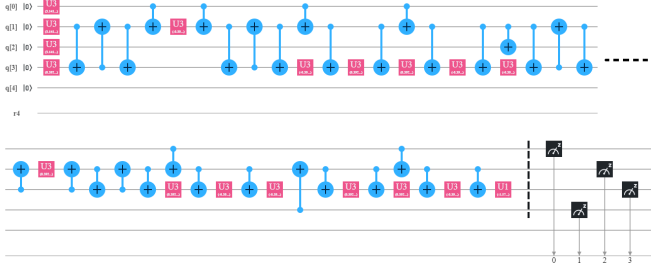


(b) Output corresponding to the input state $|1110\rangle$ after simulation on the IBMQ composer

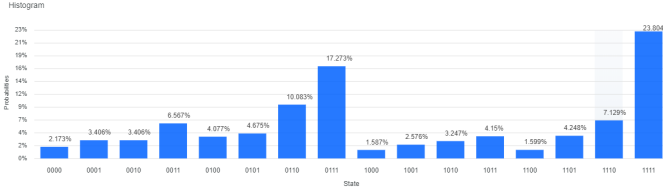
Figure 5: Decomposition of the C^3NOT gate and result of simulation in the IBMQ composer for one input $|1110\rangle$

Following the same steps sussed to decompose the Toffoli gate [11], [12], we decomposed the C^3NOT gate and it is illustrated in figure 5a. The equivalent circuit in this figure is composed by 20 CNOTs and 16 single qubits gates. The rotation gates given in stages 2, 8, 10, 16, 18, 24 and 26 of figure 5a are all identical and equal to $R_y(\pi/8)$. The single qubit gates given in stages 4, 6, 12, 14, 20, 22 and 28 of figure 5a are equal to $R_y(-\pi/8)$, the single qubit gate of stage 1 is $R_z(\pi/2)$ and it is $R_z(-\pi/2)$ for stage 30.

For an input state $|1110\rangle$, we observe with 100 % success the correct output $|1111\rangle$ in the composer (figure 5b). But for the according transpiled circuit (figure 6b), we observe the correct output only with 0.238 of success probability (figure 6a), this is basically due to the error rate of the single qubit gates and the CNOT gates, which are in the range $[3, 455 \times 10^{-4}..1.058 \times 10^{-3}]$ and $[9.144 \times 10^{-3}..1.381 \times 10^{-2}]$, respectively, according to IBMQ real device (London) [13].



(a) Output corresponding to the input state $|1110\rangle$ after execution on the IBMQ denoted *DEC* is applied to $|P_k\rangle$ and we obtain: device



(b) Transpiled decomposition of the C^3NOT gate

Figure 6: Transpiled circuit of the $CNOT$ based implementation of C^3NOT gate.

We notice that the error of the decomposition of the C^3NOT gate increases exponentially depending on the number of the CNOTs used and on the errors of all gates. We neglect in this work the errors occurring on single qubit gates and we focus on errors due to the CNOT. Therefore, we model these errors by an abstract probabilistic CNOT, denoted by $A_{CNOT}^{p,\varepsilon}$, and having the following expression [12]:

$$A_{CNOT}^{p,\varepsilon} = \begin{pmatrix} \beta_1 & \varepsilon_4 & \varepsilon_7 & \varepsilon_{10} \\ \varepsilon_1 & \beta_2 & \varepsilon_8 & \varepsilon_{11} \\ \varepsilon_2 & \varepsilon_5 & \varepsilon_9 & \beta_4 \\ \varepsilon_3 & \varepsilon_6 & \beta_3 & \varepsilon_{12} \end{pmatrix} \quad (15)$$

where $\beta = (\beta_i)_{1 \leq i \leq 4}$ represents the probability amplitude of correctly realizing the CNOT function and $\varepsilon = (\varepsilon_j)_{1 \leq j \leq 12}$ for $i, j \in \mathbb{N}^*$, are the probability amplitudes of the errors due to experimental realizations.

Let us highlight that the theoretical U_{CNOT} of equation 7 is nothing but a specific case of $A_{CNOT}^{p,\varepsilon}$ for all β_i equal to 1 and all ε_j equal to 0. This model of the errors is used to simulate the CQDRW in the next section.

III. $CNOT$ -BASED CIRCUITS FOR BUILDING CIRCULAR DISCRETE QUANTUM WALKER

A CQDRW is a quantum system described in the general form by N qubits, denoted as $[q_1..q_N]$. The qubit q_1 is used as a coin, denoted $|c\rangle$, and $N-1$ qubits $[q_2..q_N]$ are used to describe a position in a circle (Figure 7).

The walker could be in any position denoted P_k , for $0 \leq k < 2^{N-1}$, this position is represented by the state $|P_k\rangle$ in the binary form as:

$$|P_k\rangle = |p_{N-2}^k p_{N-1}^k \dots p_0^k\rangle \quad (16)$$

where $[p_{N-2}^k p_{N-1}^k \dots p_0^k]$ are specific values of qubits $[q_N q_{N-1} \dots q_2]$

The N qubits system of a CQDRW at a specific position P_k , and after performing m steps, is described by the state $|Walker_k\rangle^m$:

$$|Walker_k\rangle^m = |P_k\rangle \otimes |c\rangle = |p_{N-2}^k p_{N-1}^k \dots p_0^k\rangle \otimes |c\rangle \quad (17)$$

The walker can go one step backward or one step forward, depending on the state of the coin, being in $|0\rangle$ or $|1\rangle$, respectively. When the coin is in the state $|c\rangle = |0\rangle$, an operator

$$DEC |P_k\rangle = |P_{k-1}\rangle \quad (18)$$

When the coin is in the state $|c\rangle = |1\rangle$, an operator denoted *INC* is applied to $|P_k\rangle$ and we obtain:

$$INC |P_k\rangle = |P_{k+1}\rangle \quad (19)$$

Let us suppose the N qubits system with the CQDRW being at a specific position P_k and a coin initially at the state $|c\rangle = |0\rangle$, then equation 17 becomes:

$$|Walker_k\rangle^0 = |P_k\rangle \otimes |0\rangle = |p_{N-2}^k p_{N-1}^k \dots p_0^k\rangle \otimes |0\rangle \quad (20)$$

A single step of the walker consists of applying H transform to the coin, and then apply the appropriate *DEC* or *INC* operator depending on the state of the coin, $|Walker_k\rangle^0$ of equation 20 becomes $|Walker_k\rangle^1$:

$$\begin{aligned} |Walker_k\rangle^0 &\rightarrow |Walker_k\rangle^1 \\ &= \frac{1}{\sqrt{2}} (DEC |P_k\rangle \otimes |0\rangle + INC |P_k\rangle \otimes |1\rangle) \\ &= \frac{1}{\sqrt{2}} (|P_{k-1}\rangle \otimes |0\rangle + |P_{k+1}\rangle \otimes |1\rangle) \end{aligned} \quad (21)$$

A second step of the walker transforms equation 21 to the following:

$$\begin{aligned} |Walker_k\rangle^1 &\rightarrow |Walker_k\rangle^2 = \\ &\frac{1}{\sqrt{4}} ((DEC |P_{k-1}\rangle \otimes |0\rangle + INC |P_{k-1}\rangle \otimes |1\rangle) \\ &+ (DEC |P_{k+1}\rangle \otimes |0\rangle - INC |P_{k+1}\rangle \otimes |1\rangle)) = \\ &\frac{1}{\sqrt{4}} ((|P_{k-2}\rangle \otimes |0\rangle + |P_k\rangle \otimes |1\rangle) \\ &(|P_k\rangle \otimes |0\rangle - |P_{k+2}\rangle \otimes |1\rangle)). \end{aligned} \quad (22)$$

According to equation 22, after two steps, $|Walker_k\rangle^0$ has walked to the positions $|P_{k-2}\rangle$, $|P_{k+2}\rangle$ and returned to initial position $|P_k\rangle$, with probability amplitude equal to $1/\sqrt{4}$, $-1/\sqrt{4}$ and $1/\sqrt{2}$, respectively. For $m > 2$, we need to apply each time the transform H of equation 2, and then we apply the appropriate *DEC* or *INC* operator depending on the state of the coin $|c\rangle$. Therefore, the general state of the N qubits CQDRW, being initially at a position P_k among 2^{N-1} positions in a circle, and after performing m steps is expressed as:

$$|Walker_k\rangle^m = \sum_{i=0}^{2^m-1} \alpha_i |P_i\rangle \otimes |c\rangle \quad (23)$$

where α_i is the probability amplitude of being in the position $|P_i\rangle$ after applying the Hadamard operator m times.

A C^nNOT and a C_0^nNOT based implementation of the N qubits walker, including *DEC* and *INC* possible realization is illustrated in figure 7.

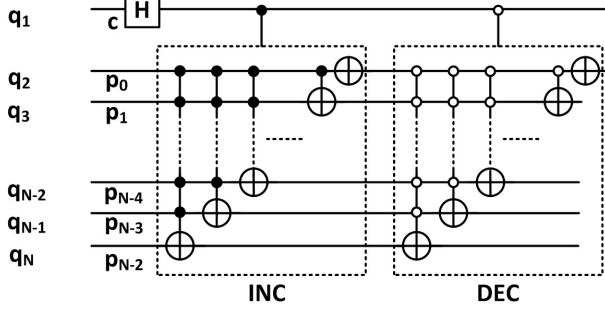


Figure 7: C^nNOT and a C_0^nNOT based implementation of N qubits CQDRW

Introducing all transformation rules presented in section 2 permits us to transform the circuit of figure 7 into a generalized single qubit and CNOT based implementation of any N qubits CQDRW.

IV. SIMULATION RESULTS

In order to study the impact of the errors of the CNOT gates on the success probability of correctly realizing the circular quantum discrete walk, we take as an example of $N = 4$ (figure 8a). An equivalent C^3NOT , C^2NOT and $CNOT$ based implementation of figure 8a is given by figure 8b. It is worth mentioning that minimization rules detailed in [10], [15] permit us to reduce the size of the circuit as given by figure 8c, but since the aim of this paper is to study the impact of the errors of the CNOT gates, we simulate the implementation of figure 8b, where we introduce the decomposition of the C^2NOT and C^3NOT , as illustrated by figures 4a and 5a, respectively.

In the specific case of $N = 4$, and for an initial position P_0 and a coin set to $|c\rangle = |0\rangle$, the initial state of the 4 qubits quantum walker is expressed as:

$$|Walker_0\rangle^0 = |P_0\rangle \otimes |0\rangle = |p_2^0 p_1^0 p_0^0\rangle \otimes |0\rangle \quad (24)$$

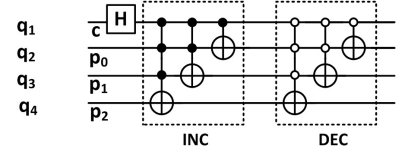
$$= |000\rangle \otimes |0\rangle$$

After one step, $|Walker_0\rangle^0$ moves to $|Walker_0\rangle^1$ as:

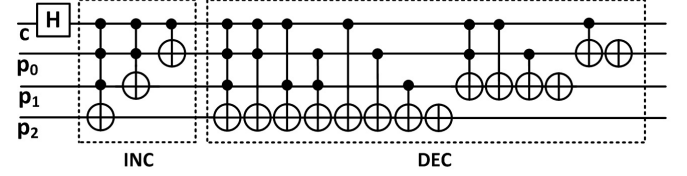
$$|Walker_0\rangle^0 \rightarrow |Walker_0\rangle^1 = \frac{1}{\sqrt{2}} (|111\rangle \otimes |0\rangle + |001\rangle \otimes |1\rangle) \quad (25)$$

The state of the walker given by equation 25 describes exactly the result obtained after simulation of the circuit on IBMQ (figure 9a). But on the real IBMQ device (figure 9b), $|Walker_0\rangle^0$ of equation 24 becomes:

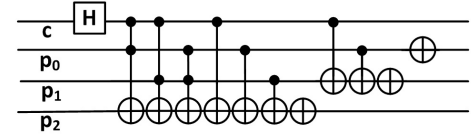
$$|Walker_0\rangle^0 \rightarrow |Walker_0\rangle^1 = \sqrt{0.1466} |111\rangle \otimes |0\rangle + \sqrt{0.0311} |001\rangle \otimes |1\rangle \quad (26)$$



(a) C^3NOT , C^2NOT , $CNOT$, C_0^3NOT , C_0^2NOT and C_0NOT based implementation

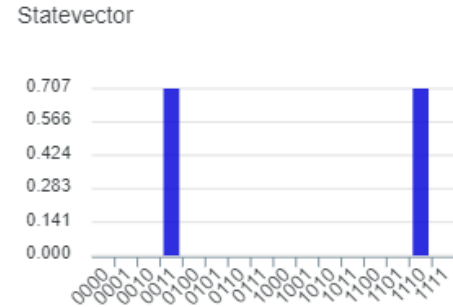


(b) C^3NOT , C^2NOT and $CNOT$ based implementation

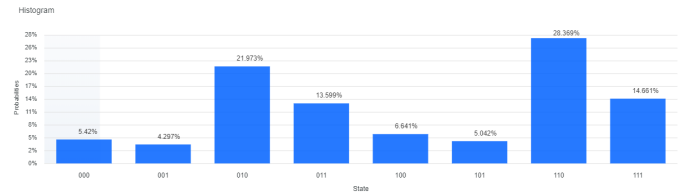


(c) Simplified circuit version of the 4 qubits walker's circuit

Figure 8: All CNOT based circuit implementation of 4 qubits CQDRW.



(a) Output corresponding to the input state $|0000\rangle$ after simulation on the IBMQ composer



(b) Output corresponding to the input state $|0000\rangle$ after execution on the IBMQ device

Figure 9: Simulation of the 4 qubits walker on IBMQ

According to equation 26 and figure 9b, we have only 0.03 and 0.14 success probabilities for ending correctly in the positions $|001\rangle$ and $|111\rangle$, after just one step of the walker. To measure the performance of the 4 qubits CQDRW over all possible initial states, we refer to the fidelity denoted \overline{F}_{Walker} and given by:

$$\overline{F}_{Walker} = \langle \Psi_{in} | U_{Walker}^\dagger \rho_t U_{Walker} | \Psi_{in} \rangle \quad (27)$$

where the upper line indicates that the fidelity is obtained according to the average over all 8 possible initial positions states $|\Psi_{in}\rangle = \{|000\rangle, |001\rangle, |010\rangle, |011\rangle, |100\rangle, |101\rangle, |110\rangle, |111\rangle\}$. ρ_t is given by $\rho_t = |\Psi_{out}\rangle\langle\Psi_{out}|$, with $|\Psi_{out}\rangle$ is the state at the output of the IBMQ transpiled 4 qubits CQDRW circuit for the specific $|\Psi_{in}\rangle$ input. The transform U_{Walker} is a 16×16 matrix representing the ideal transform of the 4 qubits CQDRW, and obtained through Matlab simulation.

The fidelity obtained by IBMQ real device is only 17.42 %. This low value is basically due to the 87 CNOTs making up the circuit (figure 8b). If we consider the error of each CNOT gate as being equal to 1.38×10^{-2} [13], the success probability of each CNOT is around 0.9862, and if we neglect the errors due to the single qubits operations and the decoherence, the total success probability of the entire circuit is approximately $\approx (0.9862)^{87} = 29.85 \%$, which is near the fidelity value obtained in our simulation.

For higher number of steps $m > 1$, the simulation of the 4 qubits CQDRW would have necessitate larger circuits and a huge number of gates. Therefore, we consider the abstract probabilistic CNOT model of equation 15, and we vary randomly all $\varepsilon = (\varepsilon_j)_{1 \leq j \leq 12}$ in a realistic range of errors $[10^{-5}..10^{-2}]$. The results of the MATLAB stimulation of the fidelity of the walker depending on these errors and on the number of steps $m = [1..50]$ (figure 10).

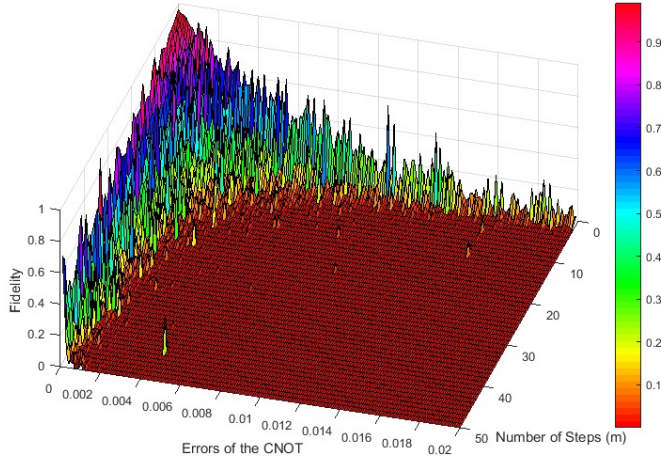


Figure 10: Fidelity of the 4 qubits CQDRW depending on the errors of the CNOT and the number of steps

According to figure 10, the fidelity value of 17.42 % obtained by IBMQ after one step, is obtained for a CNOT error around 10^{-2} , which is in the error range declared by the manufacturer. It is seen from figure 10 that reaching reasonable fidelity values around 80% or more, the error of the CNOT should be less than 10^{-4} , which leads us to conclude that actual state of the art devices are still not yet ready for simulating real quantum algorithms.

V. CONCLUSION

We investigated the CQDRW both theoretically and practically and presented a CNOT based implementation of the CQDRW in a N qubits system. We showed through simulation

on the IBMQ that the 4 qubits CQDRW system could not exceed the fidelity value of 17 %. We underlined the source of the errors is related to the number of CNOT gates used in the circuit and to the decoherence. We simulated the CQDRW for large number of steps and showed that the error of the CNOT should be lower than 10^{-4} to have acceptable fidelity values. IBMQs resources constraints limited our work to 4 qubits and informally speaking, larger CQDRW in a 5 qubits system or 2D hyper cubic quantum walks requires decomposition of the C^4NOT with more CNOTs, which will cause more and more errors. Our simulation proves that working with superconducting qubits has the major drawback of high probability of the errors. This work could be extended by proposing quantum error correcting codes used to reduce the total errors of the entire circuit.

REFERENCES

- [1] Venegas-Andraca, S. E., "Quantum walk: a comprehensive review Quantum Information Processing," 11, 1015-1106 (2012)
- [2] F. Xia, J. Liu, H. Nie, Y. Fu, L. Wan and X. Kong, "Random walk: A Review of Algorithms and Applications," in IEEE Transactions on Emerging Topics in Computational Intelligence, vol. 4, no. 2, pp. 95-107 (2020)
- [3] Douglas, B. L. and Wang, J. B. "Efficient quantum circuit implementation of quantum walk," Phys. Rev. A, 79, 052335 (2009).
- [4] Gerdali, A., Laneve, A., Bonavena, L. D., Sansoni, L., Ferraz, J., Fratalocchi, A., Sciarino, F., Cuevas, A. and Mataloni, P. "Experimental Investigation of Superdiffusion via Coherent Disordered Quantum walk," Physical review letters, 123, 140501 (2019).
- [5] Kole, A., Hillmich, S., Datta, K., Wille, R. and Sengupta, I. "Improved Mapping of Quantum Circuits to IBM QX Architectures," IEEE Transactions on Computer-Aided Design of Integrated Circuits and Systems, 1-1 (2019)
- [6] Barenco, A., Bennett, C. H., Cleve, R., DiVincenzo, D. P., Margolus, N., Shor, P., Sleator, T., Smolin, J. A. and Weinfurter, H. "Elementary gates for quantum computation," Phys. Rev. A, 52, 3457-3467 (1995).
- [7] Vedral, V., Barenco, A. and Ekert, A. "Quantum networks for elementary arithmetic operations," Phys. Rev. A, 54, 147-153 (1996).
- [8] Y. Ju, I. Tsai and S. Kuo, "Quantum Circuit Design and Analysis for Database Search Applications," in IEEE Transactions on Circuits and Systems I: Regular Papers, vol. 54, no. 11, pp. 2552-2563, (2007)
- [9] Gueddani, A., Chatta, R. and Attia, M. "CNOT-based design and query management in quantum relational databases," International Journal of Quantum Information, 12, 1450023 (2014).
- [10] Younes, A. and Miller, J. "Automated Method for Building CNOT Based Quantum Circuits for Boolean Functions," arXiv:quant-ph/0304099 (2013)
- [11] Li, C.-K., Roberts, R. and Yin X. "Decomposition of unitary matrices and quantum gates," International Journal of Quantum Information, 11, 1350015 (2013)
- [12] Shende, V. V., Bullock, S. S. and Markov, I. L. "Synthesis of quantum logic circuits," IEEE Transactions on Computer-Aided Design of Integrated Circuits and Systems, 25, 1000-1010 (2006)
- [13] <https://www.ibm.com/quantum-computing/>
- [14] Gueddani, A., Chatta, R. and Boudriga, N. "Success Probability Evaluation of Quantum Circuits Based on Probabilistic CNOT Gate," Optical Communication Systems OPTICS 2012, International Conference on, DCNET/ICE-B/OPTICS, 378-387 (2012)
- [15] Maslov, D., Dueck, G. W., Miller, D. M. and Negrevergne, C. "Quantum Circuit Simplification and Level Compaction," IEEE Transactions on Computer-Aided Design of Integrated Circuits and Systems, 27, 436-444 (2008)